

Received:
12 February 2016

Revised:
27 March 2016

Accepted:
6 July 2016

© 2016 The Authors. Published by the British Institute of Radiology under the terms of the Creative Commons Attribution-NonCommercial 4.0 Unported License <http://creativecommons.org/licenses/by-nc/4.0/>, which permits unrestricted non-commercial reuse, provided the original author and source are credited.

Cite this article as:

Lee H-J, Chung H-J, Wang H-K, Shen S-H, Chang Y-H, Chen C-K, et al. Evolutionary magnetic resonance appearance of renal cell carcinoma after percutaneous cryoablation. *Br J Radiol* 2016; **89**: 20160151.

FULL PAPER

Evolutionary magnetic resonance appearance of renal cell carcinoma after percutaneous cryoablation

^{1,2}HAN-JUI LEE, MD, ^{2,3}HSIAO-JEN CHUNG, MD, ^{1,2}HSIN-KAI WANG, MD, ^{1,2}SHU-HUEI SHEN, MD, ^{2,3}YEN-HWA CHANG, MD, PhD, ^{1,2}CHUN-KU CHEN, MD, MS, ^{2,4}HSIAO-PING CHOU, MD and ^{1,2}YI-YOU CHIOU, MD

¹Department of Radiology, Taipei Veterans General Hospital, Taipei City, Taiwan

²National Yang-Ming University School of Medicine, Taipei City, Taiwan

³Department of Urology, Taipei Veterans General Hospital, Taipei City, Taiwan

⁴Department of Radiology, Yonghe Cardinal Tien Hospital, New Taipei City, Taiwan

Address correspondence to: Dr Shu-Huei Shen

E-mail: shshen@vghtpe.gov.tw

Objective: To determine the evolutionary MRI appearance of renal cell carcinoma (RCC) following cryoablation.

Methods: For this institution review board-approved study, we recruited patients with biopsy-proven RCC and treated them with percutaneous cryoablation between November 2009 and October 2014. Two radiologists retrospectively reviewed the pre-procedural and follow-up MRI. The findings included tumour sizes, signal intensities on T_1 weighted imaging (T1WI), T_2 weighted imaging (T2WI), diffusion-weighted imaging, apparent diffusion coefficient (ADC) map and contrast enhancement patterns. The ADC values of the tumours before and after treatment were measured.

Results: A total of 26 patients were enrolled. The ablated tumours exhibited predominantly high signals on T1WI at 1-9-month follow-up (47.1% strong hyperintense at

3 months) and subsequently returned to being isointense. In T2WI, the signals of the ablated tumours were highly variable during the first 3 months and became strikingly hypointense after 6 months (58.3% strong hypointense at 6 months). Diffusion restriction was prominent during the first 3 months (lowest ADC: $0.62 \pm 0.29 \times 10^{-3} \text{ mm}^2 \text{ s}^{-1}$ at 1 month). Contrast enhancement persisted up to 6 months after the procedure. The residual enhancement gradually increased in the dynamic scan and was most prominent in the delay phase.

Conclusion: The MRI of the cryoablated renal tumour follows a typical evolutionary pattern.

Advances in knowledge: Familiarity of practitioners with the normal post-cryoablation change of RCC on MRI can enable the early detection and prevention of tumour recurrence.

INTRODUCTION

The increasing availability of ultrasound and axial image examinations implies that an increasing number of renal cell carcinomas (RCCs) are identified in the form of small, non-metastatic tumours. Using percutaneous ablation as an alternative to surgery has become widely applied in RCC treatment. Because of its minimal invasiveness and advantage of renal preserving, it is beneficial for use in patients exhibiting old age, comorbidities, an already precarious renal function, a solitary kidney and multiple or bilateral RCC or recurrent RCC.¹ Cryoablation and radiofrequency ablation for clinical T1a renal mass (≤ 4 cm) in patients with major comorbidities are recommended in American Urological Association guidelines.² Previous serial studies have proven percutaneous cryoablation for RCC to be highly effective and exhibit low complication rates.^{2,3}

The purpose for imaging follow-up after percutaneous cryoablation depends on the intervals of cryoablation. An

immediate post-procedural imaging examination (within 24 h) is typically arranged when complications are suspected. The quarterly follow-up in the first year facilitates assessing the effectiveness of the technique and detecting incomplete ablation. Consequently, timely repeated ablation can be arranged if necessary. Because higher recurrence compared with surgical excision in long-term follow-up has been reported,^{2,4} subsequent annual follow-up to prevent local recurrence is recommended.⁵

Cross-sectional images including CT and MRI have been generally adopted for post-cryoablation follow-up. Enhancement characteristics and the size of the ablation zone have been emphasized as surrogates for tumour recurrence, and the i.v. administration of the contrast material is an integral part of these examinations. The imaging evaluations usually focus on size measurement and tumour enhancement characteristics to enable assessing residual or recurrent disease.⁶ However, the enhancement after cryoablation may

persist for several months, which is undesirable for diagnosing recurrent tumours.⁷ Contrast administration is contraindicated for both CT and MR examinations in patients with impaired renal function, which is common among patients with RCC. Ultrasound contrast media have no contraindication and have been proven to be effective in post-ablation assessment; however, they are not widely available.⁸ Therefore, following up these patients by using non-contrast-enhanced cross-section imaging study is critical. Compared with non-contrast-enhanced CT, non-contrast-enhanced MR comprises various sequences and thus can provide more information regarding tissue characteristics. Understanding the evolutionary MR appearance of a treated tumour prevents misidentifying post-cryoablation change as tumour recurrence and thereby increases the sensitivity for recurrent tumour detection. The aim of this study was to determine the evolutionary change of RCC following cryoablation on MR.

METHODS AND MATERIALS

Patient selection

For this institution review board-approved retrospective study, we recruited patients with biopsy-proven RCC and treated them with image-guided percutaneous cryoablation at our institute between November 2009 and October 2014. The patients were referred for cryoablation from urologists because of contraindication or patient refusal of surgery. Routinely, these patients had undergone pre-procedural and post-procedural imaging study through CT. Patients who exhibited contraindication for contrast-enhanced CT, including renal insufficiency, were allergic to the iodine-containing contrast medium and exhibited no contraindication for the MR (e.g. pacemaker implantation) received during pre-procedural and post-procedural follow-up MR examinations. An initial 24-h follow-up after cryoablation was arranged if immediate complication was a concern. Outpatient follow-up was arranged 1 month after the procedure, quarterly within the first year and every 6 months thereafter.

Image protocol

MRI was performed using a 1.5-T MR system (Twin EXCITE, GE Healthcare, Milwaukee, WI) with an eight-channel phase-arrayed body coil. The imaging protocol for bilateral kidneys included axial unenhanced dual-echo T_1 weighted images [by T_1 weighted

imaging (T1WI)], axial T_2 weighted fast spin-echo images [by T_2 weighted imaging (T2WI)], coronal T_2 weighted single-shot fast spin-echo images, axial diffusion-weighted single-shot echoplanar imaging [diffusion-weighted imaging (DWI): repetition time/echo time = 8500 ms/minimum, matrix size = 128 × 128, field of view = 24 × 24 cm, number of excitations 4, slice thickness/gap = 4/0 mm, axial scan, b -factor values = 0 and 800 s mm⁻² for three directions of gradient and SENSE reduction factor = 2] and the corresponding apparent diffusion coefficient (ADC) map. After the injection of 0.1 mmol kg⁻¹ of gadolinium chelate (Magnevist®; Schering, Berlin, Germany) at the rate of 2 ml s⁻¹, coronal gadolinium-enhanced three-dimensional dynamic T_1 weighted images and axial gadolinium-enhanced T_1 weighted images with fat saturation were obtained. To demonstrate the enhancement in the ablation zone and to obviate the influence of high signal intensity on T1WI, subtraction images were additionally processed for the dynamic study. If the glomerular filtration rate was <30 ml/min/1.73 m², a gadolinium-containing contrast was not provided.

Tumour ablation technique

All cryoablation procedures were performed under CT guidance and monitoring by a single radiologist with 10 years' experience in interventional radiology. Patients were admitted to the ward the day before the procedure. Baseline renal function, haemoglobin and coagulation profile were checked. The procedure was performed using an angio-CT suite (Angio-CT MIYABI, Siemens, Erlangen, Germany, combining the Siemens SOMATOM® 16-slice CT on rails with the Siemens AXIOM® Multistar angiography unit) with patients lying in an orthogonal or oblique decubitus position based on the tumour location. All procedures were performed under general anaesthesia. We used an argon-based cryoablation machine and cryoablation probes (PERC-24, PERC-17; Endocare®, Irvine, CA and IceRod, IceSphere; Galil Medical, Arden Hill, MN). The numbers and types of probes were selected to achieve an appropriate ice ball shape and adequate coverage. The probes were placed at the periphery of the tumour with the distances between each probe not >2 cm. A double freeze cycle was routinely applied: 10-min freeze, followed by 10-min thawing and another 10-min freeze. During the cycle, a non-enhanced CT scan was performed at 5-min intervals (or shorter if necessary) to monitor the ice ball expansion. The shape

Table 1. Change of tumour size after percutaneous cryoablation

Change of size	24 hours	1 month	3 months	6 months	9 months	12 months	24 months	36 months
Patient number	6	7	17	12	8	10	6	5
↑↑ >10%	–	1/7	–	–	–	–	–	–
↑ <10%	2/6	3/7	1/17	–	–	–	–	–
↓ <10%	3/6	–	2/17	–	–	–	–	–
↓↓ >10%	1/6	3/7	14/17	12/12	8/8	10/10	3/3	5/5
Mean	–2%, –12~9%	–5%, –16~11%	–22%, –46~6%	–48%, –72~-19%	–45%, –71~-19%	–53%, –82~-17%	–55%, –68~-26%	–73%, –73~-45%

↑: increase of the size, ↓: decrease of the size.

and size of the ice could be controlled by changing the power and freezing time of each probe. The duration of each cycle and the power of each probe could be adjusted accordingly to prevent adjacent vulnerable organ injury or inadequate coverage.

Tumour measurement

All MR images were retrieved from hospital picture archiving and communication systems for retrospective review and comparison. The images were simultaneously reviewed by two

Table 2. Summary of the signal intensity patterns and apparent diffusion coefficient (ADC) values of the tumour before and after percutaneous cryoablation

Time point	Sequences	T1WI	T2WI	DWI	ADC ($10^{-3} \text{ mm}^2 \text{ s}^{-1}$)
Pre-procedure	Strong hyperintense	–	1/10 (10%)	–	–
	Mild hyperintense	–	2/10 (20%)	5/9 (55.6%)	1/9 (11.1%)
	Isointense	9/10 (90%)	2/10 (10%)	2/9 (22.2%)	1/9 (11.1%)
	Mild hypointense	1/10 (10%)	5/10 (50%)	2/9 (22.2%)	4/9 (44.4%)
	Strong hypointense	–	–	–	3/9 (33.4%)
					1.73 ± 0.13
24 hours	Strong hyperintense	–	–	–	–
	Mild hyperintense	–	1/6 (16.7%)	3/4 (75%)	–
	Isointense	5/6 (83.3%)	4/6 (66.6%)	1/4 (25%)	–
	Mild hypointense	1/6 (16.7%)	1/6 (16.7%)	–	3/4 (75%)
	Strong hypointense	–	–	–	1/4 (25%)
					1.15 ± 0.09
1 month	Strong hyperintense	2/7 (28.6%)	1/7 (14.2%)	2/5 (40%)	–
	Mild hyperintense	3/7 (42.8%)	2/7 (28.6%)	1/5 (20%)	–
	Isointense	2/7 (28.6%)	2/7 (28.6%)	–	–
	Mild hypointense	–	–	2/5 (40%)	2/5 (40%)
	Strong hypointense	–	2/7 (28.6%)	–	3/5 (60%)
					0.62 ± 0.29
3 months	Strong hyperintense	8/17 (47.1%)	2/17 (11.7%)	12/15 (80%)	–
	Mild hyperintense	7/17 (41.2%)	2/17 (11.7%)	3/15 (20%)	1/15 (6.7%)
	Isointense	2/17 (11.7%)	4/17 (23.5%)	–	–
	Mild hypointense	–	5/17 (29.5%)	–	4/15 (26.7%)
	Strong hypointense	–	3/17 (17.6%)	–	10/15 (66.6%)
					0.84 ± 0.22
6 months	Strong hyperintense	3/12 (25%)	–	4/10 (40%)	–
	Mild hyperintense	5/12 (41.7%)	2/12 (16.7%)	1/10 (10%)	–
	Isointense	4/12 (33.3%)	2/12 (16.7%)	1/10 (10%)	1/10 (10%)
	Mild hypointense	–	1/12 (8.3%)	2/10 (20%)	5/10 (50%)
	Strong hypointense	–	7/12 (58.3%)	2/10 (20%)	4/10 (40%)
					1.34 ± 0.31
9 months	Strong hyperintense	3/8 (37.5%)	–	1/7 (14.3%)	–
	Mild hyperintense	1/8 (12.5%)	–	2/7 (28.6%)	–
	Isointense	3/8 (37.5%)	–	–	–
	Mild hypointense	1/8 (12.5%)	4/8 (50%)	1/7 (14.3%)	5/7 (71.4%)
	Strong hypointense	–	4/8 (50%)	3/7 (42.8%)	2/7 (28.6%)
					1.67 ± 0.42

(Continued)

Table 2. (Continued)

Time point	Sequences	T1WI	T2WI	DWI	ADC ($10^{-3} \text{ mm}^2 \text{ s}^{-1}$)
12 months	Strong hyperintense	2/10 (20%)	–	1/10 (10%)	–
	Mild hyperintense	2/10 (20%)	–	4/10 (40%)	–
	Isointense	5/10 (50%)	1/10 (10%)	–	1/10 (10%)
	Mild hypointense	1/10 (10%)	4/10 (40%)	2/10 (20%)	5/10 (50%)
	Strong hypointense	–	5/10 (50%)	3/10 (30%)	4/10 (40%)
					1.39 ± 0.27
24 months	Strong hyperintense	–	–	1/6 (16.7%)	–
	Mild hyperintense	2/6 (33.3%)	–	–	–
	Isointense	4/6 (66.7%)	–	2/6 (33.3%)	1/6 (16.7%)
	Mild hypointense	–	2/6 (33.3%)	1/6 (16.7%)	4/6 (66.6%)
	Strong hypointense	–	4/6 (66.7%)	2/6 (33.3%)	1/6 (16.7%)
					1.55 ± 0.23
36 months	Strong hyperintense	–	–	–	–
	Mild hyperintense	–	–	–	–
	Isointense	5/5 (100%)	–	2/5 (40%)	1/5 (20%)
	Mild hypointense	–	2/5 (40%)	1/5 (20%)	4/5 (80%)
	Strong hypointense	–	3/5 (60%)	2/5 (40%)	–
					1.74 ± 0.42

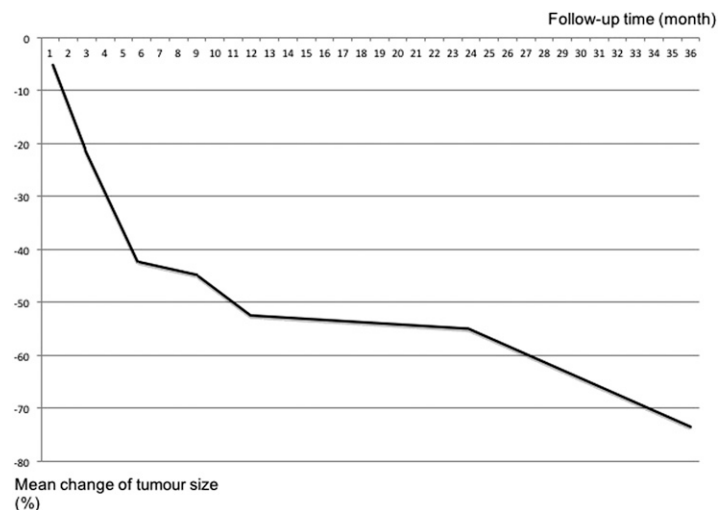
DWI, diffusion-weighted imaging; T1WI, T_1 weighted imaging; T2WI, T_2 weighted imaging.

radiologists (SHS and HJL), and one of the reviewers (SHS) was responsible for the original reporting of the MR studies. The imaging characteristics were adopted on the basis of the consensus of the two interpreting radiologists. The quantitative measurement was conducted using a standard tool available in hospital picture archiving and communication. The size of the tumour before and after ablation was measured using the maximal diameter on the axial planes according to the response evaluation criteria of solid tumours.⁹ The measurement was performed mainly on post-

contrast T_1 weighted imaging on which the ablated tumour is more easily distinguished from ablated normal renal parenchyma. The change in tumour size was calculated by dividing the diameter change (diameter of the post-ablation tumour minus the diameter of the pre-ablation tumour) by the diameter of the pre-ablation tumour.

At each follow-up MRI, the signal intensities of the ablation zone compared with the unablated normal renal parenchyma were retrospectively categorized into very hyperintense, mildly hyperintense,

Figure 1. Mean change of the ablated tumour size vs follow-up time (in months).



isointense, mildly hypointense and very hypointense on T1WI, T2WI, DWI (DWI; $b = 800$) and ADC maps. When the tumour exhibited a heterogeneous change, measurement was performed for the most prominent part. The ADC values of the tumours before and after treatment were measured. On the workstation, the regions of interest were placed on the tumour and average ADC values were acquired. On the contrast-enhanced T1WI, the enhancements of the ablated tumours, if there was any, were recorded as strong, mild or non-enhanced. The presence of viable or recurrent tumours was diagnosed if a gradually enlarged nodule within or at the periphery of the ablated tumour was noted during the two subsequent follow-up images. The signal change and contrast enhancement pattern of the recurrent tumours were recorded.

RESULTS

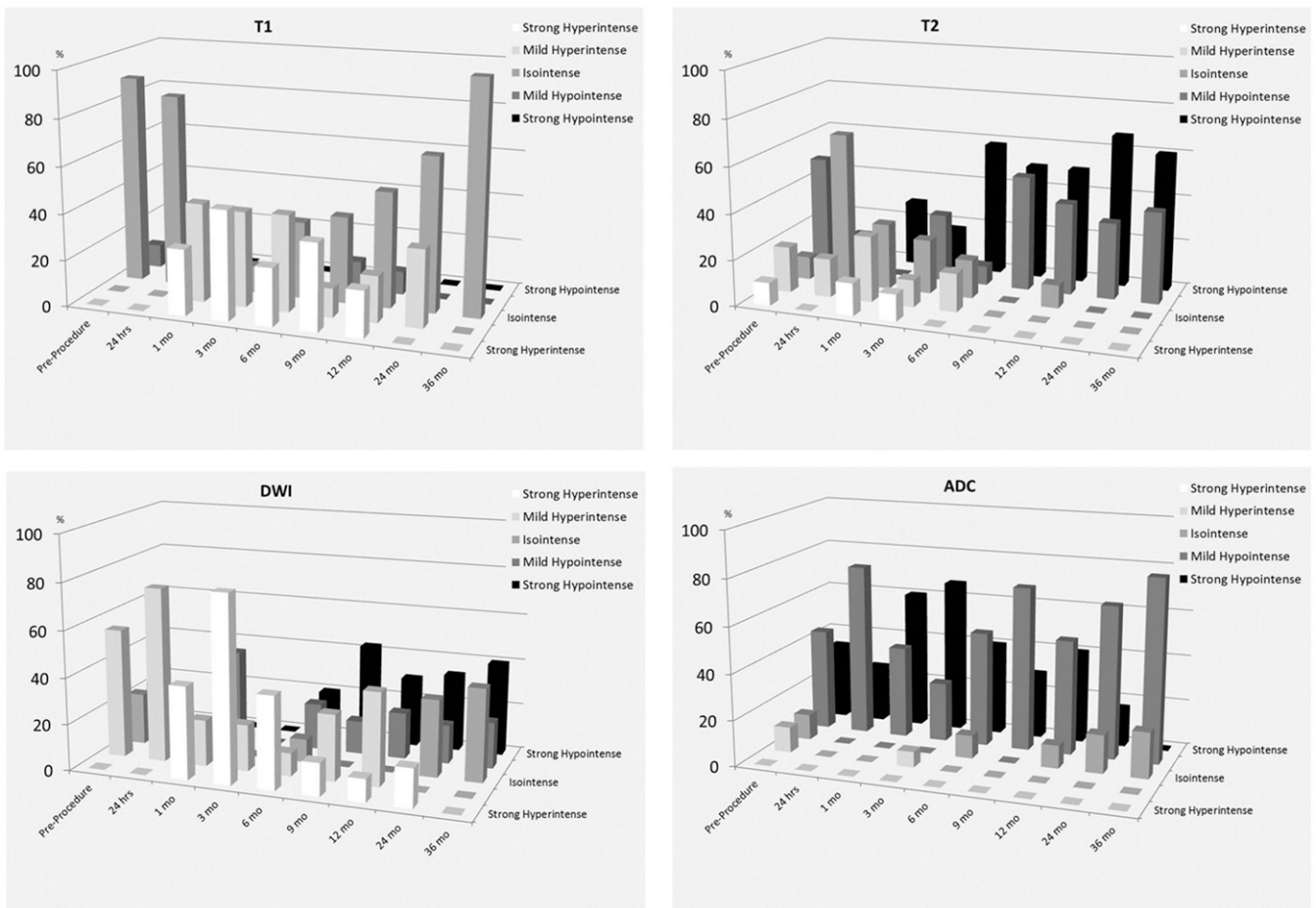
A total of 50 patients received cryoablation during the study period. 24 patients who did not receive follow-up MRI (CT was used for follow-up) were excluded. A total of 26 patients between 50 and 90 years of age (24 males and 2 females; mean age 74.2 years) were enrolled in this study. The average creatinine level of these patients was 1.4 mg dl^{-1} ($0.83\text{--}2.13 \text{ mg dl}^{-1}$), and the mean glomerular filtration rate (eGFR) was $58.4 \text{ ml/min/1.73 m}^2$ ($21\text{--}121 \text{ ml/min/1.73 m}^2$). 15 (57.7%) of the 26 patients had an eGFR of $<60 \text{ ml/min/1.73 m}^2$, among whom 14 patients

had an eGFR of $30\text{--}60 \text{ ml/min/1.73 m}^2$ and 1 patient had an eGFR of $<30 \text{ ml/min/1.73 m}^2$. Two patients did not receive biopsy because of known contralateral RCC. One patient had indeterminate biopsy results. All other patients had biopsy-proven RCC (1 chromophobe, 2 papillary and 20 clear-cell types). The mean follow-up period (from the date of cryoablation to the last OPD follow-up) was 21 months, ranging from 6 to 47 months. Not every patient regularly received an MR follow-up because of varied compliance. The number of patients receiving pre-procedural, 24-h post-procedural and 1-, 3-, 6-, 9-, 12-, 24- and 36-month follow-up MR was 10, 6, 7, 17, 12, 8, 10, 6 and 5 patients, respectively (Tables 1 and 2). One of the patients had incomplete ablation and three patients developed recurrent tumours. Two of them received repeated cryoablation, demonstrating successful local tumour control (Figure 1).

Change of tumour size

The mean tumour size before treatment was $3.1 \pm 0.9 \text{ cm}$ (range 1.6–4.0 cm). The changes of size during the follow-up are listed in Table 1 and are presented as a diagram in Figure 2. Slightly increased sizes of the ablated tumours were observed in 2 patients at 24-h follow-up [2/6 (33.3%)], in 4 patients at 1-month follow-up [4/7 (57.1%)] and in 1 patient at 3-month follow-up [1/17 (5.9%)]; the percentage of size change were mostly $<10\%$. The average size

Figure 2. Signal intensity change of the ablated tumour in the follow-up MR images. ADC, apparent diffusion coefficient; DWI, diffusion-weighted imaging; hrs, hours; mo, months.



of the ablated tumours decreased rapidly during the first 6 months. The velocity of shrinkage decelerated after 6 months and stabilized after 12 months (Figure 2).

Signal change in MR

The signal characteristics in T1WI, T2WI, DWI and ADC with corresponding ADC values are summarized in Table 2 and are presented as a bar chart in Figure 3.

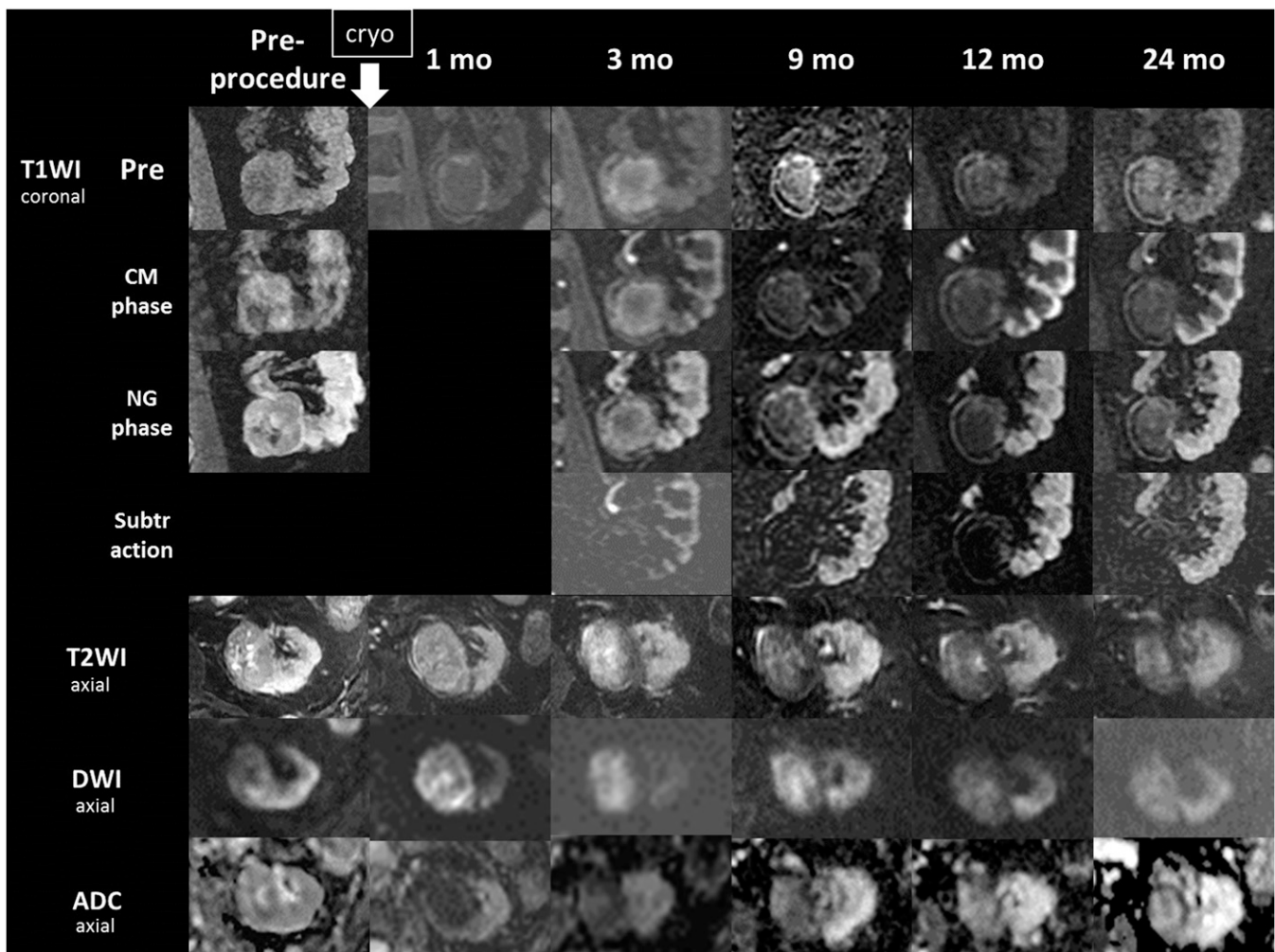
In T1WI, the ablated tumours exhibited mainly isointense signals at 24-h post-procedural MR, predominantly high signals at 1–9-month follow-up and subsequently returned to isointense signals (Figures 1 and 3–5). The change of signal intensity was usually a heterogeneous process within the tumour. A high-signal-intensity rim at the tumour margin was the most common pattern and certain tumours evolved to be homogeneous hyperintense tumours (Figures 1 and 4). Small nodular recurrences during this period

were identified as isointense or hypointense T_1 signal defects at the margin of the ablated tumour (Figures 1 and 5).

In T2WI, the signal within the ablated tumours was highly variable during the first 3 months. After 6 months, most of the tumours became considerably hypointense and subsequently persisted (Figures 1 and 3–5). A hypointense rim around the ablated area was consistently observed in all cases since the first month of treatment (Figures 1, 5 and 6b). A recurrent tumour was identified as an interruption at the hypointense rim or as a relatively hyperintense nodule within or at the periphery of the hypointense ablated tumour (Figures 1 and 5).

The pre-procedural DWI signals of the renal tumours were highly variable (55.6% hyperintense, 22.2% isointense and 22.2% hypointense), with the average ADC value being $1.74 \pm 0.42 \times 10^{-3} \text{ mm}^2 \text{ s}^{-1}$. After cryoablation, the signal intensity of

Figure 3. A 72-year-old male with coronary artery disease and chronic renal insufficiency received cryoablation (cryo) for renal cell carcinoma in the left kidney. In the follow-up images, the ablated tumour exhibited a typical evolutionary pattern including T_1 hyperintensity at 3 and 9 months, T_2 hyperintensity at 3 months, hypointensity after 9 months and a strong diffusion restriction within 9-month follow-up. The ablated tumour exhibited no enhancement in the contrast-enhanced dynamic scans. Subtraction processing enables distinguishing the high-signal-intensity background from the enhancement. ADC, apparent diffusion coefficient; CM, corticomedullary; DWI, diffusion-weighted imaging; mo, months; NG, nephrographic; Pre, pre-contrast; T1WI, T_1 weighted imaging; T2WI, T_2 weighted imaging.



the tumours gradually increased in DWI. At 3-month follow-up, all tumours were hyperintense in DWI, with 89% of them exhibiting strong hyperintensity (Figures 1, 3 and 4). The concurrent markedly low ADC values excluded the possibility of a T_2 shine-through effect ($0.62 \pm 0.29 \times 10^{-3} \text{ mm}^2 \text{ s}^{-1}$ and $0.84 \pm 0.22 \text{ mm}^2 \text{ s}^{-1}$ at 1-month and 3-month follow-up, respectively). The considerably high signal in DWI did not persist for long. It gradually decreased after 6 months and predominantly became hypointense after the 24-month follow-up. The corresponding ADC values of the tumours gradually increased (Table 2) and were mainly mildly hypointense after the 6-month follow-up.

Contrast enhancement patterns and subtraction images

The presence of contrast enhancement of the ablated tumours is listed in Table 3. Contrast enhancement was observed in half of

the tumours in the 24-h follow-up images and persisted for up to 6 months. The enhancements were rim like or nodular in shape at the periphery of the ablated tumour. They gradually increased in the dynamic study and were most prominent in the delayed phase (Figure 6c). During the first year of follow-up, because of the high-signal-intensity background of the ablated tumour in T1WI, subtraction processing enabled both confirming and excluding the contrast enhancement (Figure 4).

Residual or recurrent tumours

Four of our patients exhibited recurrence during the follow-up period (Figures 1 and 5). On T1WI, the recurrent tumours were presented as an isointense or hypointense signal defect within or at the margin of the ablated tumours, which were predominantly T_1 high SI during the first 9-month follow-up period. On T2WI, an interruption at the peripheral hypointense rim was a reliable

Figure 4. A 65-year-old male with previous left nephrectomy for renal cell carcinoma (RCC) received cryoablation (cryo) for a newly discovered RCC in the right kidney. In the 3- and 6-month follow-up images, a growing nodular lesion at the medial superior aspect of the ablated tumour was discovered, which appeared as a defect in the T_1 hyperintense and T_2 hypointense background (thin arrows). After contrast administration, the nodule exhibited an enhancement at the corticomedullary (CM) phase and washout in the nephrographic (NG) phase, indicating a recurrent tumour caused by incomplete ablation. Subsequently, secondary cryoablation was performed. At 9 months, as the previously ablated tumour exhibited a gradually reduced size and became isointense on T_1 weighted imaging (T1WI), the newly ablated part became hyperintense on T1WI (curved arrow), following a typical evolutionary pattern. ADC, apparent diffusion coefficient; DWI, diffusion-weighted imaging; mo, months; Pre, pre-contrast; T2WI, T_2 weighted imaging.

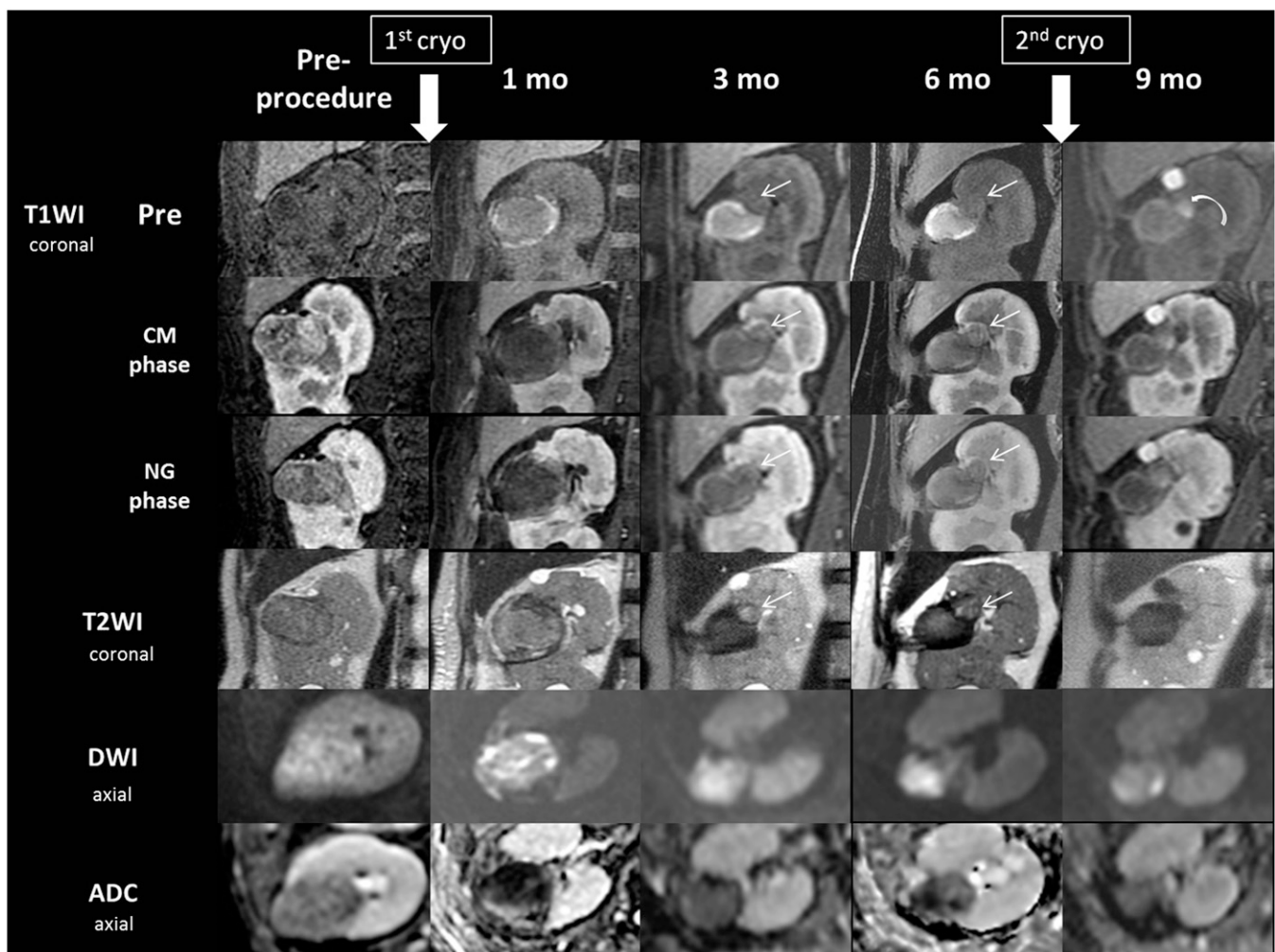
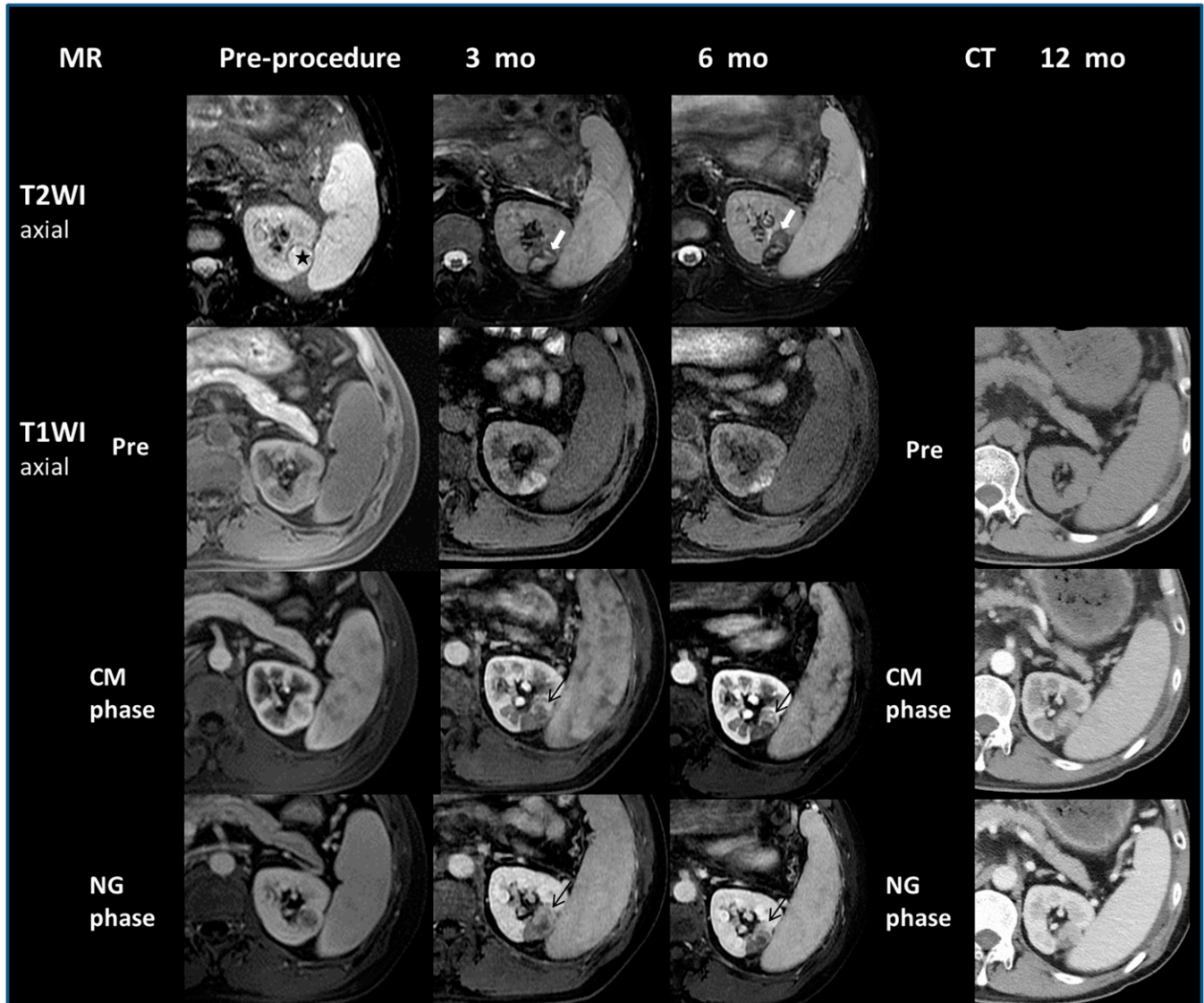


Figure 5. A 50-year-old male with hepatocellular carcinoma received cryoablation for renal cell carcinoma in the left kidney (star). The follow-up MR images at 3 and 6 months demonstrated T_1 hyperintensity of the ablated tumour with a hypointense rim on T_2 weighted imaging (T2WI). An interruption of the hypointense rim was noted at the anterior margin of the ablated tumour (thick white arrows), which was corresponding to the crescent arterial enhancement area with delay washout in the contrast-enhanced dynamic scans (thin black arrows). The CT study at 12 months showed gradual enlargement of the enhancing area, confirming the presence of tumour recurrence. CM, corticomedullary; mo, months; NG, nephrographic; Pre, pre-contrast; T1WI, T_1 weighted imaging.



indicator for tumour recurrence. After contrast administration, the recurrent tumours were presented as a crescent- or nodular-shaped enhancement at the periphery of the tumours, with arterial enhancement and delay washout pattern. In the subsequent follow-up images, a gradual enlargement of the enhancing area confirmed the presence of tumour recurrence.

DISCUSSION

Cryoablation is a recognized and effective treatment option for localized renal tumours. It is a less invasive alternative compared with surgery and is beneficial for those with a contraindication to surgery. Although several studies have shown similar oncological results between surgery and

thermal ablation,^{10,11} thermal ablation reportedly entails a higher risk of local recurrence than partial nephrectomy.¹ Previous studies have revealed that percutaneous cryoablation provides local control rates of 88–99%.^{12,13} A tumour recurrence at the margin of the tumour that occurs within 6 months implies inadequate ablation, whereas a recurrence that occurs after 6 months typically implies true local recurrence.¹⁴ A previous study reported that nearly 70% recurrence was detected within 3 months.¹⁵ Therefore, detailed image surveillance during the first year is necessary to enable the detection of early recurrence caused by incomplete ablation, so that an additional ablation procedure can be arranged in a timely manner.

Table 3. Contrast enhancement of the tumour before and after percutaneous cryoablation

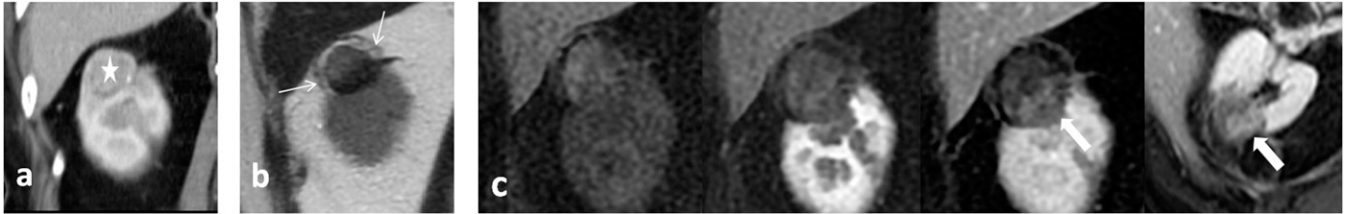
Enhancement	Pre-procedure	24 hours	1 month	3 months	6 months	9 months	12 months	24 months	36 months
Patient number	9	6	6	15	11	6	9	6	5
Strong	6/9	1/6	-	-	-	-	-	-	-
Mild	3/9	2/6	1/6	4/15	2/11	1/6	-	-	-
No	-	3/6	5/6	11/15	9/11	5/6	9/9	6/6	5/5
Subtraction	-	-	1	3	2	3	3	3	5
Necessity	-	-	1/1	2/3	2/2	3/3	2/3	0/3	0/5

The size of the ablation zone is a critical part of the evaluation in follow-up imaging. Shortly after therapy, the ablated tumour may exhibit a slightly enlarged size attributable to tissue swelling¹⁶ and gradually shrink afterwards.¹⁷ Gill et al¹⁷ reviewed the MRI appearance of tumours treated with cryoablation in 56 patients and observed a gradual involution of the ablation zone by an average of 75% after 3 years. In our observation, although several ablated tumours exhibited slightly increased sizes, the average size of the ablated tumours rapidly decreased during the first 6 months. The velocity of shrinkage decelerated after 6 months and stabilized after 12 months. The average change of size reached 73% after 36-months of follow-up. If the ablated tumour failed to follow the evolution pattern of size, locally persistent or recurrent cancer was suspected.

The post-cryoablation histopathological change follows a sequential order.¹⁸ Immediately after the procedure, a central coagulation necrosis with karyolysis, cytolysis and haemolysis was surrounded by a peripheral freeze margin with probably incomplete initial cell destruction containing pyknosis, less haemorrhage and congestion. As time progressed, the central ablated area revealed fibrous granulation, dystrophic calcifications and haemosiderin deposition. The peripheral margin formed a fibrous granulation capsule. The cryoimmunologic response began through the release of cytokines and chemokines from the damaged cells, initiated infiltration of inflammatory cells and underwent tissue repair. Thus, the survival cells within the freeze target processed delayed or secondary necrosis for a period of days or weeks.^{19,20} The MRI appearance of cryolesions demonstratively reflected orderly histopathological findings in a rabbit model.²⁰ An earlier study by Remer et al²¹ described sequential MRI findings in 21 patients after cryoablation. However, it was based on an earlier generation involving a liquid nitrogen-based system, not the argon-based system that is currently widely adapted worldwide. The study described the trend of the ablated tumours of being isointense on T1WI and isointense or hypointense on T2WI within the first year, whereas information about functional sequences including DWI and the dynamic contrast enhancement pattern was not available.

In this study, we comprehensively described the imaging appearance of RCC post-cryoablation by using T1WI, T2WI and DWI scans. The non-contrast-enhanced MRI followed a regular sequential evolutionary pattern in the first year. In contrast to the study of Remer et al,²¹ we found that the ablated tumours that exhibited high signal intensity were most prominently rim shaped in T1WI during the first follow-up year and were most prominent during the first 1–9 months. This signal intensity is consistent with previous observations and may be attributable to the variable central coagulation, necrotic processes and inflammatory responses.^{18,22} Tumour recurrence during this period may be detected as an isointense or hypointense T_1 signal defect within or at the margin of the ablated tumour. In T2WI, the signal within the ablated tumours was highly variable during the first 3 months. At 6 months, most of the tumours became considerably hypointense and subsequently persisted. A possible cause is that the inflammatory response aided in the removal of the necrotic tissue and a fibrous scar replaced the ablated tumour.^{19,20} Dense hypointense rims around the ablated area

Figure 6. A 70-year-old male with previous partial nephrectomy for renal cell carcinoma: (a) post-contrast CT coronal reconstruction imaging revealed a locally recurrent tumour (star), which was subsequently treated by cryoablation. (b) In the 3-month follow-up MRI, the tumour was hypointense on T_2 weighted imaging with a dense hypointense rim (thin arrows). (c) After contrast administration (from left to right: coronal pre-contrast phase, coronal corticomedullary phase, coronal nephrographic phase and axial delay phase), the medial posterior part of the ablated tumour exhibited a gradual nodular enhancement (thick arrows). The enhancement disappeared in the subsequent follow-up images (not shown).



(not the tumour) were consistently observed in all cases since the first month after treatment. The finding may correspond to the scarring and fibrosis at the freeze margin^{20,21} and can be used to evaluate the adequacy of the ablation area, and a recurrent tumour may be regarded as an interruption at the hypointense rim. We found T2WI to be a useful sequence for detecting recurrent tumour. Either interruption of the hypointense rim or a relatively hyperintense area in the hypointense background of the ablated area after 6-month follow-up can be the presentation of tumour recurrence.

DWI of renal tumour after cryoablation has not been reported. Chen et al²³ described the low ADC values of the cryoablated region in the canine prostate in MRI performed immediately after cryoablation. After 53 days, the treated regions exhibited increased ADC values and a proliferation of scar tissue.²⁴ In our study, the pre-procedural DWI and ADC values of the tumour were highly variable (Table 2). However, considerably high signals in DWI were consistently observed in the first 3 months with corresponding low ADC values, indicating a true diffusion restriction. This might be related to the observed tissue swelling. The signal of DWI became markedly hypointense beginning at the 6–9-month follow-up, which may histologically correspond to the scar formation at a later stage.¹⁹

Abnormal nodular- or crescent-shaped areas of contrast enhancement within the ablated area have been considered to indicate a residual or recurrent tumour of the renal cell after thermal ablation.²⁵ Furthermore, in the absence of these findings, CT density measurement in Hounsfield units can provide further information. Ideally, the enhancement of the ablation zone should not exceed 10 HU.²⁶ However, diagnosing tumour viability according to enhancement is problematic. The residual enhancement at the ablated tumour has been adequately described in cryoablation literature. Recent studies have suggested that tumours may exhibit enhancement immediately after ablation, which may persist for up to 3–6 months after cryoablation, and is usually heterogeneous, nodular or peripheral rim like in shape.^{17,18} Stein et al⁷ reviewed 32 tumours treated with cryoablation. The results showed persistent enhancement in 15% of the cases at 3 months, which persisted for up to 9 months, leading to unnecessary surgery. The follow-up imaging for patients with

renal insufficiency for whom iodinated contrast agents and gadolinium are contraindicated remains unclear. In this study, the contrast enhancement persisted up to 6 months. The dynamic enhancement pattern of the residual enhancement differs from that of residual and recurrent tumours. The residual enhancement gradually increased in the dynamic scan and was most prominent in the delay phase, which differs from the most common arterial enhancement and delay washout enhancement pattern of RCCs. The T_1 hyperintensity of the ablated tumour during the 1–9-month follow-up can be easily misconstrued as enhanced tissue. Post-processing by subtraction could remove the effects and thus help in both detecting and excluding contrast enhancement.

This study has several limitations. The number of cases is small, and it was a retrospective study. It is unknown whether there is interobserver variability of the MR findings investigated because the two radiologists reviewed the images and made a consensus together. The follow-up interval of the patients did not completely follow the planned schedule and thus, longitudinal comparisons in the same patients were impossible. The tumours diagnosed as recurrent tumours were not pathologically proven. Neither were those diagnosed to have stable disease. However, a sufficient follow-up time may enable excluding the possibility of tumour recurrence. Further study involving more patients and prospective observation may confirm our findings.

In conclusion, percutaneous cryoablation is a procedure that is less invasive than surgery and constitutes an effective treatment for RCC. Cross-sectional imaging follow-up has been used as the surrogate for local tumour recurrence. For patients contraindicated to i.v. contrast injection, non-contrast-enhanced MR is a critical tool for follow-up in treating cryoablated tumours. In this study, we demonstrated that MRI of the ablated renal tumour follows a typical evolutionary pattern. Familiarity with the normal post-ablation change is required to detect tumour recurrence early and prevent misconstruing normal post-ablation change as a recurrent tumour.

FUNDING

This study was supported by a research grant from the NSC grant number NSC101-2314-B-075-050.

REFERENCES

- Allen BC, Remer EM. Percutaneous cryoablation of renal tumors: patient selection, technique, and postprocedural imaging. *Radiographics* 2010; **30**: 887–900. doi: <http://dx.doi.org/10.1148/rg.304095134>
- Campbell SC, Novick AC, Beldegren A, Blute ML, Chow GK, Derweesh IH, et al. Guideline for management of the clinical T1 renal mass. *J Urol* 2009; **182**: 1271–9. doi: <http://dx.doi.org/10.1016/j.juro.2009.07.004>
- Cornelis F, Balageas P, Le Bras Y, Rigou G, Boutault JR, Bouzgarrou M, et al. Radiologically-guided thermal ablation of renal tumours. *Diagn Interv Imaging* 2012; **93**: 246–61. doi: <http://dx.doi.org/10.1016/j.diii.2012.02.001>
- Kunkle DA, Egleston BL, Uzzo RG. Excise, ablate or observe: the small renal mass dilemma—a meta-analysis and review. *J Urol* 2008; **179**: 1227–33; discussion 1233–4. doi: <http://dx.doi.org/10.1016/j.juro.2007.11.047>
- Goldberg SN, Grassi CJ, Cardella JF, Charboneau JW, Dodd GD 3rd, Dupuy DE, et al; Society of Interventional Radiology Technology Assessment Committee; International Working Group on Image-Guided Tumor Ablation. Image-guided tumor ablation: standardization of terminology and reporting criteria. *Radiology* 2005; **235**: 728–39. doi: <http://dx.doi.org/10.1148/radiol.2353042205>
- Ganguli S, Brennan DD, Faintuch S, Rayan ME, Goldberg SN. Immediate renal tumor involution after radiofrequency thermal ablation. *J Vasc Interv Radiol* 2008; **19**: 412–8. doi: <http://dx.doi.org/10.1016/j.jvir.2007.10.024>
- Stein AJ, Mayes JM, Mouraviev V, Chen VH, Nelson RC, Polascik TJ. Persistent contrast enhancement several months after laparoscopic cryoablation of the small renal mass may not indicate recurrent tumor. *J Endourol* 2008; **22**: 2433–9. doi: <http://dx.doi.org/10.1089/end.2008.0261>
- Meloni MF, Bertolotto M, Alberzoni C, Lazzaroni S, Filice C, Livraghi T, et al. Follow-up after percutaneous radiofrequency ablation of renal cell carcinoma: contrast-enhanced sonography versus contrast-enhanced CT or MRI. *AJR Am J Roentgenol* 2008; **191**: 1233–8. doi: <http://dx.doi.org/10.2214/AJR.07.3238>
- Eisenhauer EA, Therasse P, Bogaerts J, Schwartz LH, Sargent D, Ford R, et al. New response evaluation criteria in solid tumours: revised RECIST guideline (version 1.1). *Eur J Cancer* 2009; **45**: 228–47. doi: <http://dx.doi.org/10.1016/j.ejca.2008.10.026>
- Tanagho YS, Bhayani SB, Kim EH, Figenshau RS. Renal cryoablation versus robot-assisted partial nephrectomy: Washington University long-term experience. *J Endourol* 2013; **27**: 1477–86. doi: <http://dx.doi.org/10.1089/end.2013.0192>
- Long CJ, Kutikov A, Canter DJ, Egleston BL, Chen DY, Viterbo R, et al. Percutaneous vs surgical cryoablation of the small renal mass: is efficacy compromised? *BJU Int* 2011; **107**: 1376–80. doi: <http://dx.doi.org/10.1111/j.1464-410X.2010.09851.x>
- Georgiades C, Rodriguez R. Renal tumor ablation. *Tech Vasc Interv Radiol* 2013; **16**: 230–8. doi: <http://dx.doi.org/10.1053/j.tvir.2013.08.006>
- Lai WJ, Chung HJ, Chen CK, Shen SH, Chou HP, Chiou YY, et al. Percutaneous computed tomography-guided cryoablation for renal tumor: experience in 30 cases. *J Chin Med Assoc* 2015; **78**: 308–15. doi: <http://dx.doi.org/10.1016/j.jcma.2014.12.006>
- Atwell TD, Callstrom MR, Farrell MA, Schmit GD, Woodrum DA, Leibovich BC, et al. Percutaneous renal cryoablation: local control at mean 26 months of followup. *J Urol* 2010; **184**: 1291–5. doi: <http://dx.doi.org/10.1016/j.juro.2010.06.003>
- Matin SF, Ahrar K, Cadeddu JA, Gervais DA, McGovern FJ, Zagoria RJ, et al. Residual and recurrent disease following renal energy ablative therapy: a multi-institutional study. *J Urol* 2006; **176**: 1973–7. doi: <http://dx.doi.org/10.1016/j.juro.2006.07.016>
- Bolte SL, Ankem MK, Moon TD, Hedican SP, Lee FT, Sadowski EA, et al. Magnetic resonance imaging findings after laparoscopic renal cryoablation. *Urology* 2006; **67**: 485–9. doi: <http://dx.doi.org/10.1016/j.urology.2005.09.015>
- Gill IS, Remer EM, Hasan WA, Strzempkowski B, Spaliviero M, Steinberg AP, et al. Renal cryoablation: outcome at 3 years. *J Urol* 2005; **173**: 1903–7. doi: <http://dx.doi.org/10.1097/01.ju.0000158154.28845.c9>
- Porter CA 4th, Woodrum DA, Callstrom MR, Schmit GD, Misra S, Charboneau JW, et al. MRI after technically successful renal cryoablation: early contrast enhancement as a common finding. *AJR Am J Roentgenol* 2010; **194**: 790–3. doi: <http://dx.doi.org/10.2214/AJR.09.2518>
- Baust JG, Gage AA, Bjerklund Johansen TE, Baust JM. Mechanisms of cryoablation: clinical consequences on malignant tumors. *Cryobiology* 2014; **68**: 1–11. doi: <http://dx.doi.org/10.1016/j.cryobiol.2013.11.001>
- Zhu Q, Shimizu T, Abo D, Jin M, Nagashima K, Miyasaka K. Magnetic resonance imaging findings and histopathological observations after percutaneous renal cryoablation in the rabbit model. *J Urol* 2006; **175**: 318–26. doi: [http://dx.doi.org/10.1016/S0022-5347\(05\)00009-1](http://dx.doi.org/10.1016/S0022-5347(05)00009-1)
- Remer EM, Weinberg EJ, Oto A, O'Malley CM, Gill IS. MR imaging of the kidneys after laparoscopic cryoablation. *AJR Am J Roentgenol* 2000; **174**: 635–40. doi: <http://dx.doi.org/10.2214/ajr.174.3.1740635>
- Tatli S, Acar M, Tuncali K, Sadow CA, Morrison PR, Silverman SG. MRI assessment of percutaneous ablation of liver tumors: value of subtraction images. *J Magn Reson Imaging* 2013; **37**: 407–13. doi: <http://dx.doi.org/10.1002/jmri.23827>
- Chen J, Daniel BL, Diederich CJ, Bouley DM, van den Bosch MA, Kinsey AM, et al. Monitoring prostate thermal therapy with diffusion-weighted MRI. *Magn Reson Med* 2008; **59**: 1365–72. doi: <http://dx.doi.org/10.1002/mrm.21589>
- Butts K, Daniel BL, Chen L, Bouley DM, Wansapura J, Maier SE, et al. Diffusion-weighted MRI after cryosurgery of the canine prostate. Magnetic resonance imaging. *J Magn Reson Imaging* 2003; **17**: 131–5. doi: <http://dx.doi.org/10.1002/jmri.10227>
- Gervais DA, Arellano RS, McGovern FJ, McDougal WS, Mueller PR. Radiofrequency ablation of renal cell carcinoma: part 2, lessons learned with ablation of 100 tumors. *AJR Am J Roentgenol* 2005; **185**: 72–80. doi: <http://dx.doi.org/10.2214/ajr.185.1.018500072>
- Gervais DA, McGovern FJ, Wood BJ, Goldberg SN, McDougal WS, Mueller PR. Radio-frequency ablation of renal cell carcinoma: early clinical experience. *Radiology* 2000; **217**: 665–72. doi: <http://dx.doi.org/10.1148/radiology.217.3.r00dc39665>